

Improvement in the sustainability and stability of acrylic protective coatings for outdoor bronze artworks

G. Pellis^a, B. Giussani^b, P. Letardi^c, T. Poli^a, P. Rizzi^a, B. Salvadori^d, A. Sansonetti^e, D. Scalrone^{a,*}

^a Department of Chemistry, University of Torino, Via Pietro Giuria 7, Torino, Italy

^b Science and High Technology Department, Università degli Studi dell'Insubria, Via Valleggio 9, Como, Italy

^c Institute of Anthropic Impacts and Sustainability in the Marine Environment, CNR, Via De Marini 6, Genova, Italy

^d Institute of Heritage Science, CNR, Via Madonna del Piano 10, Sesto Fiorentino, Italy

^e Institute of Heritage Science, CNR, Via Roberto Cozzi 53, Milan, Italy

ARTICLE INFO

Keywords:

Metal protection
Corrosion inhibitors
Light stabilizers
Photooxidation
Heritage
Conservation

ABSTRACT

Outdoor bronze artworks are an entrenched part of our urban landscape. They are usually covered by a patina resulting from their exposition to the environment. This patina plays an important aesthetic role and may provide some passivation on the surface, nonetheless it does not prevent the degradation processes promoted by external factors such as pollution, light and humidity. One of the strategies to slow down these unwanted processes is the application of protective coatings. The products currently available have some limitations due to the loss of effectiveness over time and poor environmental sustainability. With the aim of proposing more performing alternatives, coatings based on Paraloid® B44 modified with corrosion inhibitors and light stabilizers were prepared and characterized. Two non-toxic corrosion inhibitors were studied, 5-mercapto-1-pheniltetrazole (MPT) and 5-ethyl-1,3,4-thiadiazol-2-amine (AEDTA), comparing them with the traditional benzotriazole (BTA). The approach used aimed to identify the blend providing the most stable coatings. The chemical and physical properties of the coatings, such as colour, solubility, glass transition and composition, were studied and monitored over time. All coatings have shown adequate visual properties; however, corrosion inhibitors degrade some other properties of the coatings and need to be used in conjunction with light stabilizers. The permanence of corrosion inhibitors in the coatings over time was also studied by investigating the role of the support. The establishment of specific interactions between inhibitors and the bronze surface lengthens their permanence in the coatings compared to what happens with inert supports. Especially for AEDTA, the inhibitor retention within the coating and at the coating-bronze interface is better than for BTA and MPT.

The effect of each of the additives on the photooxidation stability of the coating was evaluated and the most promising inhibitor and stabilizer combination was identified.

1. Introduction

The conservation of metal art objects is a complex and demanding task, especially for those placed outdoors and exposed to atmospheric agents and reactive compounds present in the environment [1,2]. Rain, abrasive agents such as windblown sand and debris, air pollution, and human contact are just few of the main responsible for the degradation of metal artworks [3,4]. In particular, the complex nature of the surfaces of outdoor bronze artworks is a major challenge for their conservation, and proper methodologies should be adopted to address the interaction with the environment so as to preserve them for future generations [4,

5]. The most difficult task is in balancing the preservation of the so called “noble patina” surface layer and to protect the surface of the bronze artwork from detrimental interaction with the environment. Indeed, “noble patina”, with its pleasant appearance, is part of the heritage aesthetic value and slows down the corrosion rate with respect to bare metal. Unfortunately, this kind of patina is not stable enough in the changing environment, with pollutants and physical-chemical parameters which may lead to remarkable alteration of the composition and appearance of the surface layer [6]. As a matter of fact, the most widespread common practice for the protection of outdoor bronze monuments consists in the application of coatings on the surface [7]

* Corresponding author.

<https://doi.org/10.1016/j.polyimdegradstab.2023.110575>

Received 16 September 2023; Accepted 21 October 2023

0141-3910/© 2023 The Author(s). Published by Elsevier Ltd. This is an open access article under the CC BY license (<http://creativecommons.org/licenses/by/4.0/>).

which should be renewed when the protective properties become too weak. In general, coatings for conservation are applied to avoid the contact between the metal-patina layers and the actively corroding agents present in the environment. Treatments applied to heritage assets must meet specific requirements [4,8]. An ideal sustainable coating should prevent the object from degradation without modifying its appearance: in this view, only transparent colourless coatings are allowed. Moreover, the chemical nature of the treatments should permit their removal with a safe and non-toxic approach. Eventually, the properties of these treatments should assure a total compatibility with the surfaces involved, a good protective effectiveness, long-term durability and low-cost maintenance [1,8]. Nowadays, the most used protective products are waxes and Inralac®, but both present problems: Inralac® contains benzotriazole (BTA)[2,9,10], a harmful corrosion inhibitor, suspected of being carcinogenic and which is released into the environment over time, while waxes are easily deteriorated by the environment they are supposed to protect the artworks from [11,12]. The actual conservation perspective focuses on new eco-friendly and safe treatments to overcome the drawbacks of Inralac® or waxes, even though the latter are still considered very attractive options. In the last 20 years, the most tested protective coatings for copper and its alloys have been functional coatings with triazoles, silanes and fluoropolymers [11–15]. More recently, other innovative solutions have been taken into account as well, like nano-composites and biopolymers [4,7]. Finally, preliminary studies outlined promising results concerning the application of different inorganic coatings based on calcium oxalates [16] and diamond-like carbon, applied by plasma-enhanced chemical vapour deposition [18]. Although the initial outcomes are encouraging, several aspects related to effectiveness and durability must be further explored to implement tailored applications of these systems as protective coatings for Cultural Heritage.

In this research, Paraloid® B44-based coatings containing a non-toxic corrosion inhibitor and a light stabilizer are investigated. The choice of Paraloid® B44 relies on its peculiar properties of being transparent, versatile, exhibiting strong adhesion, stability and long term reversibility making it an ideal protective coating specifically recommended for metal protection [19]. Two types of commercially available corrosion inhibitors have been studied: 5-mercapto-1-phenyltetrazole (MPT) and 5-ethyl-1,3,4-thiadiazol-2-amine. (AEDTA) [15, 17]. They have already been tested for bronze protection, providing encouraging results, but so far they have been rarely used as components for polymer coatings. Their toxicity profile is safer than that of BTA, involving less restrictions on their usage. However, a limitation of corrosion inhibitors is represented by their light-sensitivity and their poor persistence within the coating [20,21]. Consequently, light stabilisers were added aiming at preventing the corrosion inhibitors and the acrylic resin from photooxidative degradation. Two stabilizers were chosen based on their different mechanisms of action: the UV absorber Tinuvin® 312, (i.e. N'-(2-ethoxyphenyl)-N-(2-ethylphenyl)oxamide) and Tinuvin® 5050, a mixture of UV absorber (i.e. 2-(2-hydroxyphenyl) benzotriazole) and a HALS-Hindered Amine Light Stabilizer. The solvent used to solubilize the various components and prepare the coatings is 1-methoxypropan-2-ol, a solvent with low toxicity [22].

The proposed coatings were characterized by applying a multi-analytical protocol to investigate their intrinsic properties and the feasibility of their application on bronze specimen simulating artworks. Furthermore, the same multi-analytical protocol was applied on Inralac® films which were used as a reference product. To assess the coating stability over time, the prepared specimens underwent artificial solar ageing and their structural and compositional changes were monitored by Fourier Transformed Infrared Spectroscopy (FTIR). Colour stability was evaluated by colorimetric measurements. Differential Scanning Calorimetry (DSC) was used to determine the glass transition temperature (T_g) and to estimate other properties of the coatings such as adhesion, mechanical resistance and flexibility. Reversibility was assessed by determining the insoluble fraction of the coatings after

ageing. Moreover, the persistence of corrosion inhibitors in the coatings was studied by Pyrolysis-Gas Chromatography /Mass Spectroscopy (Py-GC/MS). Finally, four coatings were selected and applied by brush on bronze mock ups. Their chemical changes during artificial solar light irradiation were monitored through μ FTIR in reflection mode.

2. Experimental

2.1. Materials

The components of the coatings prepared and analysed in this research are listed in Table 1. Paraloid® B44 (ethyl acrylate/methyl methacrylate copolymer) was purchased from Sinopia s.a.s. The corrosion inhibitor 5-mercapto-1-phenyltetrazole (MPT) was purchased from Alfa Aesar and 5-ethyl-1,3,4-thiadiazol-2-amine (AEDTA) from Sigma Aldrich. Tinuvin® 312 (N'-(2-ethoxyphenyl)-N-(2-ethylphenyl)oxamide) and Tinuvin® 5050 (a mixture of 2-(2-hydroxyphenyl) benzotriazole and a HALS) were obtained from BASF. The solvent used to solubilize the various components and prepare the coatings was 1-methoxypropan-2-ol purchased from Sigma Aldrich (Table 1). The solutions were prepared by adding the various ingredients in a vial in the following order: acrylic resin, additives and finally the solvent. They were stirred for 24 h until complete solubilization. The solutions were applied with a brush or poured with the aid of a pipette on different flat supports and left to dry until complete solvent evaporation and formation of a thin solid film. Glass slides, silicon wafers, a white ceramic tile and bronze discs were used as supports, depending on the type of analysis to be performed, as summarised in Table 2. To ensure maximum reproducibility of the characteristics of the coatings, they were applied on the various supports in a controlled way: for FTIR analysis on silicon wafers the thickness of the coatings was controlled by assuring that the absorbance of the most intense peak was between 0.7 and 1; for coatings prepared on glass slides the quantity of solid coating per surface unit was kept constant by adjusting the volume of solution spread on the glass; for coatings applied by brush, the same brush was used both for white tile and bronze discs. On the white tile the application was performed by two strokes in the same direction while for bronze discs two strokes were made orthogonally, to ensure the whole covering of the surface.

The inhibitors were tested in three different concentrations, while a fixed concentration was used for light stabilizers. The composition of the prepared solutions and of the dried coatings obtained after solvent evaporation are reported in Table 3 and 4, respectively.

The coatings were aged for 1000 h in a Q-Sun Xe-1 Xenon Test Chamber (Q-Lab Corporation, UK), at constant temperature of 50°C, irradiance set at 0.68 W/m² at 340 nm and Daylight Q filter (cut-on at 295 nm), simulating exposure to direct sunlight. They were regularly monitored by colorimetric measurements and FTIR spectroscopy, while DSC, Py-GC/MS and the determination of the insoluble fraction were performed before and after aging. The same analyses were also carried out on Inralac®.

2.2. Characterization

2.2.1. Colour measurements

Colour measurements were performed to assess colour stability of the coatings over time. The change of colour (ΔE^*_{ab}) was calculated for each area comparing the colour coordinates L*, a*, b* obtained before and after aging. The colour difference has been computed according to the parameter ΔE^*_{ab} , which represents the Euclidean distance between the two colours (CIELAB1976):

$$\Delta E^*_{ab} = \sqrt{(\Delta a^*)^2 + (\Delta b^*)^2 + (\Delta L^*)^2}$$

In the three-dimensional CIELAB colour space L* defines the lightness and it goes from 0 (black) to 100 (white), a* is a chromatic scale in the green (negative values) - red (positive values) direction and b* is the

Table 1
Structures of the coating components.

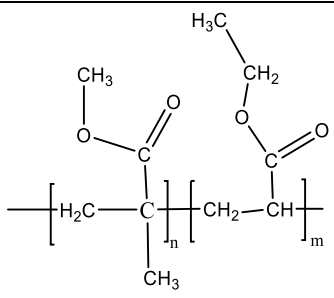
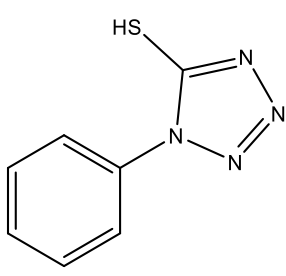
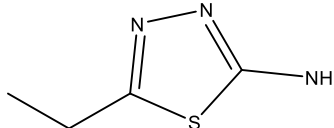
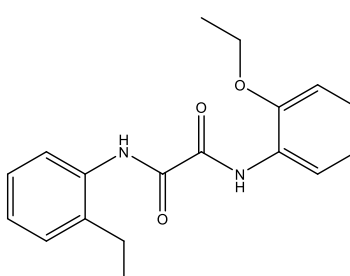
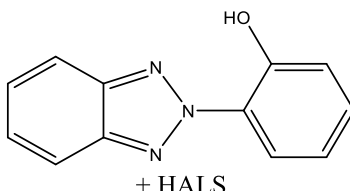
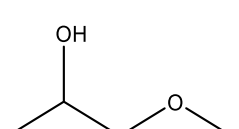
Name	Structure
Paraloid® B44 ethyl acrylate/methyl methacrylate copolymer	
MPT 5-mercapto-1-phenyltetrazole	
AEDTA 5-ethyl-1,3,4-thiadiazol-2-amine	
Tinuvin® 312	
Tinuvin® 5050	 + HALS
1-methoxypropan-2-ol	

Table 2
Application method of the coating and type of support used depending on the analysis.

Application method of the coating and type of support	Techniques					
	Colorimetry	FT-IR	μFTIR	Py-GC/MS	DSC	Insoluble fraction
Poured on glass slide				X	X	X
Poured on silicon wafer		X				
By brush on white ceramic tile	X					
By brush on bronze discs			X			

chromatic scale blue (negative values) to yellow (positive values). Thin coatings were applied by brush on a white tile and analysed by a Portable Spectrophotometer CM-700d KONICA Minolta in SCI (Specular Component Included) mode; For each mock-up, colour coordinates L^* , a^* and b^* were acquired for a total of 15 measurements (5 sites of measure, 3 measurements for each site) then the average values were calculated.

2.2.2. Fourier Transform Infrared Spectroscopy (FTIR)

FTIR was used for chemical characterization and to monitor chemical changes over time. All coatings were applied on silicon supports and analysed in transmission mode with a Perkin Elmer Spectrum 100 spectrometer equipped with a DTS detector. Each analysis was performed carrying out 16 scans in a range from 450 cm^{-1} to 4500 cm^{-1} , with a resolution of 4 cm^{-1} . For reflectance micro-FTIR analyses a Spotlight FTIR Perkin Elmer microscope with a MCT detector was used collecting 32 scans per spectrum, at 2 cm^{-1} resolution in the range between 650 cm^{-1} to 4000 cm^{-1} .

2.2.3. Differential Scanning Calorimetry (DSC)

DSC provided the glass transition temperature of the coatings. The samples needed for the analysis were taken with a scalpel by scratching the coatings applied on glass slides. The analyses were performed with a Q200 (TA Instruments) Differential Scanning Calorimeter (DSC) and were carried out on 8 mg of sample (unaged and aged), setting a heat-cool-heat cycle from -20°C to 110°C with a ramp of $10^\circ\text{C}/\text{min}$ under nitrogen flow.

2.2.4. Insoluble fraction

The insoluble fraction was determined to get information on the coating reversibility. The coatings were prepared on microscope slides in six replicas. Three of them were aged and the others were used to determine the percentage of insoluble fraction before ageing. The microscope slides were weighted before and after the application of the coating, during and after the artificial ageing. The insoluble fraction was determined after having soaked the films in tetrahydrofuran and having collected it with a vacuum filtration system on pre-weighted PTFE membrane filters ($0.45\text{ }\mu\text{m}$). Data reported are the average of the three replicas.

2.2.5. Pyrolysis-gas chromatography/mass spectrometry (Py-GC/MS)

Py-GC/MS analyses were used to assess the stability of corrosion inhibitors and their persistence in the coatings over time. The analyses were performed in double-shot mode with a micro-furnace Multi-Shot Pyrolyzer EGA/Py-3030D (Frontier Lab, Japan) coupled to a GC/MS system. Samples were placed into a stainless-steel cup and inserted into the micro-furnace. For the first shot the pyrolysis temperature was set at 250°C and kept for 1 minute. In the second shot the sample was pyrolyzed at 500°C for 12 seconds. The interface temperature of the pyrolyzer was 280°C and the temperature of the GC injector was kept at 280°C .

Table 3

Composition of the solutions [%w/w].

	Sample number																				
	1	2	3	4	5	6	7	8	9	10	11	12	13	14	15	16	17	18	19	20	21
B44	10	10	10	10	10	10	10	10	10	10	10	10	10	10	10	10	10	10	10	10	10
AEDTA	/	/	/	/	/	/	/	/	/	/	/	/	1.0	0.5	0.1	1.0	0.5	0.1	1.0	0.5	0.1
MPT	/	/	/	1.0	0.5	0.1	1.0	0.5	0.1	1.0	0.5	0.1	/	/	/	/	/	/	/	/	/
TIN312	/	0.3	/	/	/	0.3	0.3	0.3	0.3	/	/	/	/	/	/	0.3	0.3	0.3	/	/	/
TIN5050	/	/	0.3	/	/	/	/	/	/	0.3	0.3	0.3	/	/	/	/	/	/	0.3	0.3	0.3
1-methoxypropan-2-ol	90.0	89.7	89.7	89	89.5	89.9	88.7	89.2	89.6	88.7	89.2	89.6	89	89.5	89.9	88.7	89.2	89.6	88.7	89.2	89.6

Table 4

Composition of dry coatings [%w/w].

	Sample number																				
	1	2	3	4	5	6	7	8	9	10	11	12	13	14	15	16	17	18	19	20	21
Coating Label	B	BT3	BT5	M9	B	M5	M1	M9	B	M1	M9	B	B	B	A1	A9	A5	A1	B	B	B
Composition (% w/w)	B44	100	97	91	95	99	88	92	96	88	92	96	91	95	99	88	92	96	88	92	96
AEDTA	/	/	/	/	/	/	/	/	/	/	/	/	9	5	1	9	5	1	9	5	1
MPT	/	/	/	9	5	1	9	5	1	9	5	1	/	/	/	/	/	/	/	/	/
TINUVIN 312	/	3	/	/	/	/	3	3	3	/	/	/	/	/	/	3	3	3	/	/	/
TINUVIN 5050	/	/	3	/	/	/	/	/	/	3	3	3	/	/	/	/	/	/	3	3	3

The GC was equipped with a methylphenyl-polysiloxane cross-linked 5% phenyl methyl silicone (30 m, 0.25 mm i.d., 0.25 μm film thickness) capillary column. The carrier gas was helium (1.0 mL/min) and split ratio was 1/20 of the total flow. The following temperature program was used for the gas chromatographic separation: isotherm of 2 minutes at 50°C, ramp of 10°C/min up to 300°C, isotherm at 300°C for 10 minutes. An Agilent 8860 Gas Chromatograph and a 5977B Mass Selective Detector (Agilent Technologies, USA) were used. Mass spectra were recorded under electron impact at 70 eV, scan range 45–800 m/z. All instruments were controlled by Agilent Mass Hunter Workstation (ver. 10.1.49) software. The mass spectra assignment was done by mass library searches (NIST2008), by comparison with literature data and interpretation of fragmentation paths of mass spectra.

3. Results and Discussion

Since one of the most important prerequisites of coatings for the protection of bronze sculptures and objects is preserving the aspect of the artwork, a colorimetric study was performed in order to evaluate whether the application of the coatings could influence the appearance of the works of art. Fig. 1 shows the colour changes of the different coatings applied by brush on a white tile after 1000 h of ageing under artificial solar light. The results obtained were encouraging, as they highlight that the colour change (ΔE) of all coatings is below the threshold of perceptibility for the human eye ($\Delta E=3$, in red) [23]. In detail, although the variations are slight, all the samples show negative values of ΔL^* and positive values of Δb^* , respectively suggesting a darkening and a yellowing of the surface. The most negative ΔL^* values occur in Incralac® and Paraloid® B44, alone or with MPT, while blends containing MPT always have more positive Δb^* values than blends with AEDTA (see Table 1S on Supplementary Material). According to Fig. 1, blends with MPT show much less colour stability with respect to AEDTA; in general, higher concentration of inhibitor corresponds to somehow greater colour change, although MPT do not strictly follow this trend. Also, the influence of light stabilisers is not the same for the two tested inhibitors: Tinuvin® 5050 provides a slightly better colour stability for both AEDTA and MPT at all tested concentrations, while Tinuvin® 312 increases the colour change upon weathering for AEDTA blends and shows the opposite effect for the MPT blends. It is worth noting that Incralac® showed a ΔE higher than or equal to all the other tested coatings except Paraloid® B44 with 9% w/w of MPT, while the blends with AEDTA show a much better colour stability with respect to both Incralac® and Paraloid® B44 alone.

To evaluate the possible effect of the additives on the thermal and mechanical stability of the coatings, the glass transition temperature (T_g) of the differently formulated coatings were compared. Flexibility or stiffness, strength or brittleness depend on the glass transition

temperature, which in turn affects both the adhesion to the surfaces and the integrity and continuity of the coatings. Specifically, an increase in T_g caused by radical cross-linking reactions of the polymer during photooxidative degradation [24–26] could result in a greater brittleness of the coating, with formation of cracks and loss of adhesion.

The increase in the T_g values of the coatings after ageing with respect to T_g of the as prepared samples are reported in Fig. 2. Although well-defined trends are not always identified, it is nonetheless possible to make some general observations. As expected, the T_g of Paraloid® B44 has a limited increase during aging. Both MPT and AEDTA cause an increase in T_g and therefore a stiffening and embrittlement of the coatings during ageing. However, the addition of light stabilizers reduces the increase of the T_g and ensures greater stability of the thermal and mechanical properties. This stabilizing effect was observed for both types of Tinuvin®.

The T_g data are well correlated with the amount of insoluble cross-linked fraction present in the aged coatings (Fig. 3). Both MPT and AEDTA cause an increase in the insoluble fraction, which makes the removability of the coatings more problematic in case it becomes necessary. However, the trend in the formation of insoluble fraction as a function of the concentration of inhibitor is opposite: the amount of insoluble fraction of MPT-coatings increases inversely proportional to the concentration of the inhibitor, becoming particularly relevant at minimum concentration of MPT, whereas AEDTA increases the amount of insoluble fraction proportionally to its concentration. Moreover, regardless of the type of inhibitor, light stabilizers inhibit the degradation reactions that cause the formation of cross-linked and insoluble acrylic fractions, confirming the effect already demonstrated by the study of the glass transition temperature of the coatings. From this point of view, the coatings containing AEDTA and a light stabilizer are the ones with the best performances, since their solubility and removability remain unchanged.

To chemically characterize the coatings, ATR-FTIR analyses of the coatings and of their single components were carried out. All the assignments were done referring to literature data. Paraloid® B44 absorptions are the main peaks in all spectra: the CH_3 asymmetric stretching at about 2988 cm^{-1} , the CH_2 asymmetric stretching at 2952 cm^{-1} , the C=O stretching at about 1732 cm^{-1} , the CH_3 and CH_2 asymmetric bending at 1478 and 1449 cm^{-1} respectively, the CH_3 symmetric bending and CH_2 wagging at 1386 cm^{-1} and the C-O-C stretching vibrations in the range between 1300 and 1100 cm^{-1} [27–29] (Fig. 4, red curve).

FTIR peaks of the anticorrosive agent AEDTA are detected in the range from 3400 cm^{-1} to 3000 cm^{-1} , due to NH stretching, at 1637 cm^{-1} , due to N-H deformation vibration of the primary amine, at 1538 and 1524 cm^{-1} , due to characteristic vibrations of the thiazole ring (Fig. 4, blue curve).

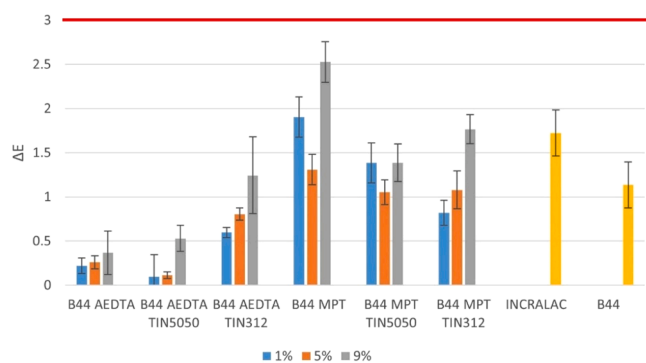


Fig. 1. Colour change of the coatings after artificial ageing. The blue, orange and grey bars refer to the concentration of the corrosion inhibitors MPT and AEDTA at 1, 5 and 9% w/w, respectively. Error bars refer to standard deviation.

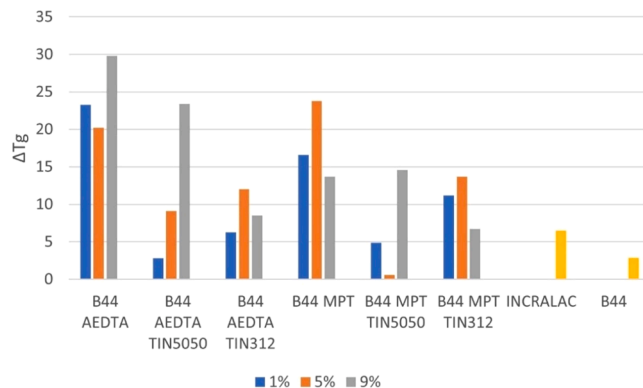


Fig. 2. ΔT_g values before and after ageing of the coatings. The blue, orange and grey bars refer to the concentration of the corrosion inhibitors MPT and AEDTA at 1, 5 and 9% w/w, respectively.

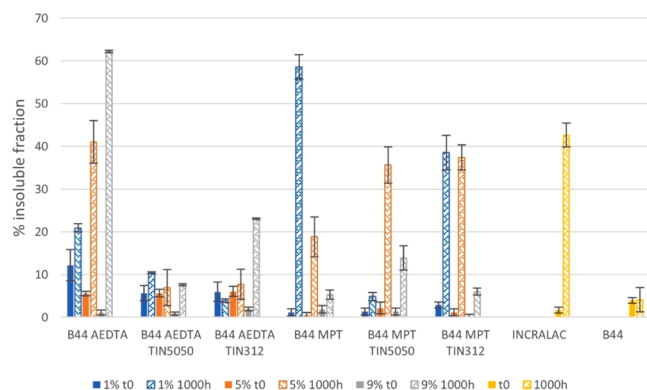


Fig. 3. Insoluble fraction of Paraloid® B44 coatings modified with corrosion inhibitors AEDTA and MPT. The blue, orange and grey bars refer to the concentration of the corrosion inhibitors MPT and AEDTA at 1, 5 and 9% w/w, respectively. Error bars refer to standard deviation.

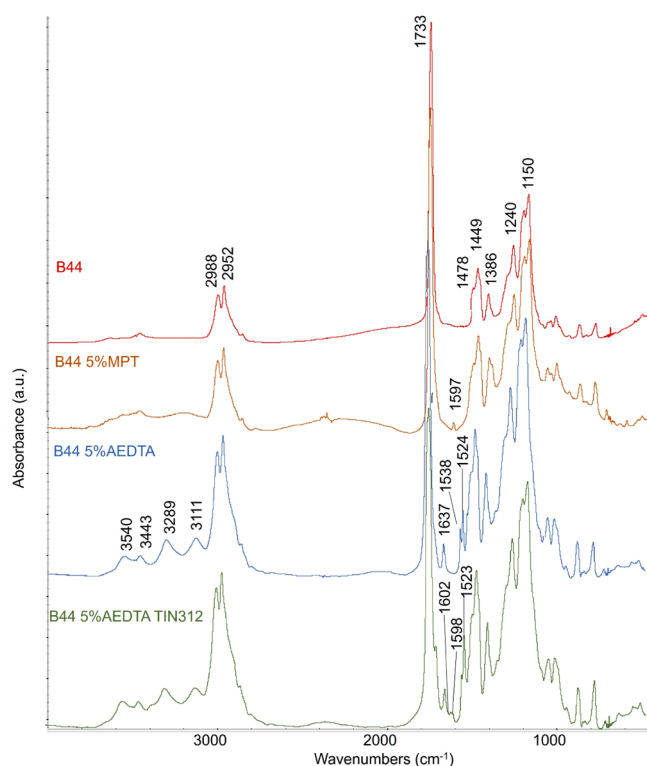


Fig. 4. FTIR spectra of coatings made of Paraloid® B44, Paraloid B44 and 5% w/w MPT, Paraloid® B44 and 5% w/w AEDTA, Paraloid® B44 added with 5% w/w AEDTA and Tinuvin® 312.

The characteristic peaks of Tinuvin® 312 are visible at 1602, 1591 and 1523 cm^{-1} (Fig. 4, green curve), while no specific signals of Tinuvin® 5050 can be identified in the FTIR spectra of the coatings. The only visible signal of the anticorrosive agent MPT is the peak at 1597 cm^{-1} , assigned to the C=C stretching (Fig. 4, yellow curve).

Thus, specific peaks of Paraloid® B44 and the corrosion inhibitors were identified, allowing for the monitoring of structural changes and persistence of the additives during the accelerated light aging of the coatings. This was undertaken by studying the spectral variations over the entire spectral range after normalization of the spectra, assuming that the absorption of the CH_3 bending vibration at 1385 cm^{-1} remained constant over time [30]. Following this procedure, no significant variations in the absorptions of the acrylic component of the coatings were observed, which indicates a good photo-oxidative stability of Paraloid®

B44, as such and with additives.

To shed a light on the fate of corrosion inhibitors over time, the change in intensity of their characteristic peaks in FTIR spectra were monitored. Fig. 5 shows a detail of the spectra of the coatings with 5% w/w of corrosion inhibitors AEDTA and MPT. The red boxes in the Fig. highlight the range of wavenumbers in which the corrosion inhibitors absorb.

Both characteristic peaks of AEDTA in the spectral range 3100–3600 cm^{-1} and the peaks at 1638, 1538 and 1524 cm^{-1} disappear over time (Fig. 5, left) indicating a decrease of the additive likely due to its degradation or migration to the coating surface and volatilization. The same also happens in coatings containing MPT whose characteristic peak at 1597 cm^{-1} also decreases during aging (Fig. 5, right).

The possible effect of light stabilizers on the persistence of corrosion inhibitors was also investigated. The persistence of AEDTA was found to be increased in coatings containing the UV absorber Tinuvin® 312. As a matter of fact, AEDTA characteristic peak at 1632 cm^{-1} is observed also at 1000 h of ageing (Fig. 1S, Supplementary Material). On the contrary, Tinuvin® 5050 seems to have no effect on the persistence of AEDTA which after a while disappears from the coating or at least is no longer detectable by FTIR. Similarly, Tinuvin® 5050 did not provide any improvement to the persistence of MPT in the acrylic coatings.

On the other hand, FTIR spectra could not clarify if Tinuvin® 312 is able to increase the stability of MPT because the characteristic FTIR peaks of MPT and Tinuvin® 312 absorb exactly in the same range of wavenumbers preventing any conclusion on possible effects of the UV absorber on the amount of corrosion inhibitor retained in the coating. So, according to FTIR analyses, Paraloid® B44 is stable to light ageing, whereas the corrosion inhibitors tend to leave the coating over time. In addition, Tinuvin® 5050 is not able to extend the permanence of the inhibitors in the coatings.

To further investigate the stability of corrosion inhibitors, double-shot Py-GC/MS analyses were performed on unaged and aged coatings. The double shot approach allowed a clearer distinction and identification of additives from the acrylic component: according to this method, the first shot consists in the thermal desorption and detection of the volatile fraction of the sample, while, during the second shot at higher temperature, the polymeric component is pyrolyzed and analysed. This helped in a better understanding of the stability and persistence of the additives in the coatings. Both coatings containing only corrosion inhibitors and those including corrosion inhibitors and light stabilisers were investigated and compared to Inralac®.

Table 5 reports the assignments of the main chromatographic peaks eluted after thermal desorption and Table 6 resumes the main peaks identified during the pyrolysis step of double-shot Py-GC/MS analyses of Paraloid® B44 coatings modified with AEDTA, MPT and light stabilisers.

In Fig. 6 the chromatograms of the thermal desorption step of the coating containing Paraloid® B44, 5% w/w AEDTA and 3% w/w Tinuvin® 312 (BA5T3 in Table 5) before (a) and after 1000 h of light aging (b) are compared. In both chromatograms AEDTA is detected in its molecular unaltered form at elution time of about 13.96 min (peak 21); neither degradation products nor pyrolytic fragments are observed. This highlights AEDTA stability under thermal and UV stress. Tinuvin® 312, namely N'-(2-ethoxyphenyl)-N-(2-ethylphenyl)oxamide, is eluted at 25.70 min (peak 39), and other marker peaks, all by-products due to Tinuvin® 312 fragmentation in the desorption step, are detected at 11.25 min (i.e. 2-ethoxyaniline, peak 13), at 24.70 min (i.e. N,N'-bis(2-phenylethyl)oxamide, peak 37) and at 26.63 min (i.e. N,N'-bis(2-ethoxyphenyl)oxamide, peak 40). These markers are detected both at time zero and after 1000 h of ageing, confirming the light stability of Tinuvin® 312.

In Fig. 7 the chromatograms obtained in the desorption step of unaged and aged Paraloid® B44 coatings with 5% w/w AEDTA and 3% w/w Tinuvin® 5050 are shown. Again, AEDTA is detected at 13.96 min (peak 21) in both chromatograms, while the main marker peaks of Tinuvin® 5050, that are bis(2,2,6,6-tetramethylpiperidin-4-yl)

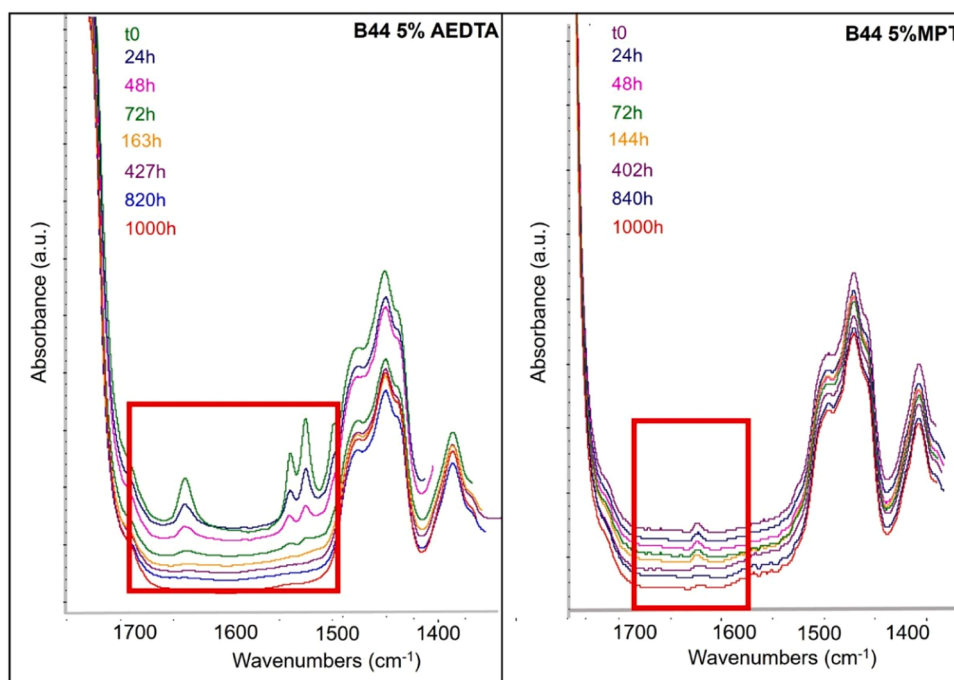


Fig. 5. Detail of Paraloid® B44 coatings with 5% w/w AEDTA (left) and 5% w/w MPT (right). Red boxes highlight corrosion inhibitors absorption peaks.

decanedioate (peak 36), bis(1,2,2,6,6-pentamethylpiperidin-4-yl) decanedioate (peak 38) and peaks 41 and 42, are not detected or have very different intensity in the aged coatings, indicating a poor stability of Tinuvin® 5050 under UV stress.

Differently from AEDTA, MPT is affected by a consistent fragmentation during the desorption step (Fig. 8). In fact, even in the unaged sample, MPT is not detected as such, but in the form of fragments and molecular adduct: isocyanatobenzene (peak 7) at 6.47 min, aniline (peak 8) at 6.85 min, isothiocyanatobenzene (peak 11) at 10.70 min, methyl(phenyl)cyanamide at 12.38 (peak 16), phenylcyanamide at 13.73 (peak 20) and methylated MPT at 17.23 min (peak 28). Fragments 7, 8, 11, 16 and 20 can be also found in the aged samples but relatively less abundant in comparison to the other components. Conversely methylated MPT disappears during aging and is replaced by 1-phenyltetrazole at about 15.44 min (peak 25). Overall, the changes observed in the MPT marker peaks following exposure to artificial sunlight indicate that this inhibitor is not stable to photooxidative aging. The behaviour of the two light stabilizers in the presence of MPT is confirmed, i.e. Tinuvin® 312 is stable under the artificial aging conditions adopted, while Tinuvin® 5050 is no longer found in aged coatings.

Similarly, the analyses carried out on Inralac® also highlighted the almost complete disappearance of BTA in the aged coatings (Table 2S and Fig. 2S, Supplementary Material), confirming what is known about the poor persistence of benzotriazole in Inralac® [31].

As for the pyrolysis step at 500°C (Table 6), it caused the expected fragmentation of the acrylic resin. At lower retention times the two most intense peaks are referable to the two structural units of Paraloid® B44, i.e. EA at 2.23 min and MMA at 2.52 min. Added to these, there are two pyrolysis by-products, MA and EMA. At higher retention times, the main peaks are assigned to sesquimers, dimers and trimers of acrylic and methacrylic units. The chromatograms of the second shot of the Py-GC/MS analyses do not show significant differences between the various types of coatings, nor between aged and unaged coatings.

To further study the permanence of corrosion inhibitors in the coating and to investigate a possible effect of the support, mock ups were prepared by applying coatings containing 5% w/w corrosion inhibitors and 3% w/w Tinuvin® 312 on the surface of polished bronze discs (i.e. bronze covered with the thin native oxide formed immediately after

exposing the reduced metal to air). Micro-FTIR analyses highlighted that in coatings with MPT the corrosion inhibitor was still present and clearly detected even after 1000 h of artificial ageing (Fig. 3S, Supplementary Material), suggesting a higher affinity for the bronze surface rather than for glass. This confirms the preferential interaction of the corrosion inhibitor with bronze and suggests that adsorption of MPT on the metal surface can occur not only when the inhibitor is applied alone [32], but also when it is applied as an additive to an acrylic coating. The preferential interaction of MPT with the bronze surface slows the loss of inhibitor from the coating over time, compared to inert surfaces such as glass.

As regards the coatings containing AEDTA, surprisingly, the micro-FTIR spectra did not show, even in the unaged coating, the characteristic absorption peak of AEDTA at 1637 cm^{-1} . This is in contrast to what was observed in coatings applied on glass slides. The same, albeit with a different inhibitor, had already been observed by Giuliani *et al.* [33] who also demonstrated the formation of a layer of inhibitor concentrated at the bronze-coating interface. Accordingly, the coating was peeled off the bronze disc and spectra were collected all over the exposed surface of the bronze. The spectra thus obtained were characterized by all the significant peaks of AEDTA (Fig. 9). This result indicates that most of AEDTA is located on the surface of the coating in contact with bronze, which makes it difficult to detect the inhibitor directly through FTIR reflection analyses. At the same time, the formation of an AEDTA layer at the coating-bronze interface is something positive as it ensures the presence of the anticorrosion additive right on the surface on which it is expected to act.

4. Conclusions

The photo-oxidative stability of Paraloid® B44 coatings containing sustainable corrosion inhibitors and light stabilizers, as well as their ability to retain the inhibitors in the film longer than currently commercial products, were investigated. All the coatings modified with AEDTA showed negligible colour changes over time, a highly desirable feature as protective coatings for cultural heritage must not alter the visual aspect of the artwork. On the other hand, coatings containing MPT were homogeneous and transparent but with a clear tendency to

Table 5
Assignment of the chromatographic peaks detected in the thermal desorption step of the double-shot Py-GC/MS analyses. (See Table 4 for coating labels).

Peak nr	Tr (min)	Assignment	DESORPTION STEP																			
			t0										1000h									
			B	B	B	B	B	B	B	B	B	B	B	B	B	B	B	B	B	B	B	B
			A9	A5	A9	A5	A5	M9	M5	M9	M5	M5	A9	A5	A9	A5	A5	M9	M5	M9	M5	M5
T3	T3	T5	T5		T3	T3	T5	T5		T3	T3	T5	T5		T3	T3	T5	T5				
1	1.28	1-methoxypropan-2-ol	X	X	X	X	X	X	X	X	X	X	X	X	X	X	X	X	X	X		
7	6.47	Isocyanatobenzene						X	X	X	X	X					X	X	X	X		
8	6.85	Aniline						X	X	X	X	X					X	X	X	X		
9	9.80	1-ethyl-2-isocyanatobenzene						X									X	X				
10	9.98	2-ethylaniline	X	X									X	X								
11	10.70	Isothiocyanatobenzene						X	X	X	X	X					X	X	X	X		
12	10.98	(methyltrisulfanyl)methane						X	X	X								X				
13	11.23	2-ethoxyaniline	X	X				X	X				X	X				X				
14	11.78	Sesquimer EA/MMA	X		X	X	X	X	X	X	X				X	X						
16	12.38	Methyl(phenyl)cyanamide						X	X	X	X	X							X	X		
18	12.52	Dimer EA	X	X	X	X	X	X	X	X	X	X	X	X	X							
19	12.98	3-methylquinoline																		X		
20	13.73	Phenylcyanamide						X	X	X	X						X	X	X	X		
21	13.96	5-ethyl-1,3,4-thiadiazol-2-amine	X	X	X	X	X						X	X	X	X	X					
22	14.96	2,6-ditert-butyl-4-methylphenol	X	X	X	X	X															
24	15.44	1-phenyltetrazole								X									X	X		
25	15.50	m/z 57,70, 74, 129, 156, 157, 185													X							
26	16.1	1,3-benzothiazol-2-amine						X	X	X								X	X	X		
27	16.46	Dimethyl decanedioate			X	X				X					X	X			X			
28	17.23	1-methyl-4-phenyltetrazole-5-thione						X	X	X	X	X				X	X					
29	17.83	Trimer EA MMA MMA	X	X	X	X	X	X	X	X	X		X	X	X					X		
30	18.01	Trimer EA MMA MMA	X	X	X	X	X	X	X	X	X				X	X						
32	18.60	Trimer EA	X	X	X	X	X	X	X	X	X				X	X						
33	18.81	m/z 57, 70, 74, 129, 156, 157, 185											X	X	X	X						
35	20.96	Octathiocane						X	X	X	X	X										
36	23.50	bis(2,2,6,6-tetramethylpiperidin-4-yl) decanedioate			X	X				X	X				X	X						
37	24.70	N,N'-bis(2-phenylethyl)oxamide	X	X				X	X				X	X			X	X				
38	24.78	Bis(1,2,2,6,6-pentamethylpiperidin-4-yl) decanedioate			X	X				X	X											
39	25.7	N'-(2-ethoxyphenyl)-N-(2-ethylphenyl)oxamide	X	X				X	X				X	X			X	X				
40	26.64	N,N'-bis(2-ethoxyphenyl)oxamide	X	X				X	X				X	X			X	X				
41	29.35	Marker of Tinuvin® 5050			X	X				X	X				X	X						
42	31.31	Marker of Tinuvin® 5050			X	X				X	X											
43	32.72	Marker of Tinuvin® 5050			X	X				X	X				X	X			X	X		
44	33.35	Marker of Tinuvin® 5050			X	X				X	X				X	X			X	X		
45	33.70	Marker of Tinuvin® 5050			X	X				X	X				X	X			X	X		
46	34.00	Marker of Tinuvin® 5050			X	X				X	X				X	X			X	X		

Table 6
Assignment of the chromatographic peaks detected in the pyrolysis step of the double-shot Py-GC/MS analyses. (See Table 4 for coating labels).

Peak nr	tr (min)	Assignment	PYROLYSIS STEP																																
			t0										1000h																						
			B	A9	T3	B	A5	T5	B	A5	T5	B	M9	T3	B	M5	T5	B	M5	T3	B	M9	T3	B	M5	T5	B	M9	T3	B	M5	T5			
2	2.10	Methyl prop-2-enoate (MA)	X			X			X			X			X			X			X			X			X			X			X		
3	2.71	Ethyl prop-2-enoate (EA)	X			X			X			X			X			X			X			X			X			X			X		
4	2.88	Methyl 2-methylprop-2-enoate (MMA)	X			X			X			X			X			X			X			X			X			X			X		
5	3.83	Ethyl 2-methylprop-2-enoate (EMA)	X			X			X			X			X			X			X			X			X			X			X		
6	9.04	Dimethyl 2-methylidenebutanedioate	X			X			X			X			X			X			X			X			X			X			X		
9	9.80	1-ethyl-2-isocyanatobenzene	X			X			X			X			X			X			X			X			X			X			X		
14	11.78	Sesquimer EA-MMA	X			X			X			X			X			X			X			X			X			X			X		
17	12.40	m/z 169, 154, 141, 125, 109, 81, 73	X			X			X			X			X			X			X			X			X			X			X		
18	12.52	EA dimer	X			X			X			X			X			X			X			X			X			X			X		
23	14.95	2,6-di-tert-butyl-4-methylphenol	X			X			X			X			X			X			X			X			X			X			X		
29	17.83	Trimer EA-FA-MMA	X			X			X			X			X			X			X			X			X			X			X		
30	18.01	Trimer EA-FA-MMA	X			X			X			X			X			X			X			X			X			X			X		
31	18.20	m/z 200, 167, 153, 135, 127, 107, 95	X			X			X			X			X			X			X			X			X			X			X		
32	18.60	Trimer EA	X			X			X			X			X			X			X			X			X			X			X		
34	18.82	m/z 268, 255, 200, 149, 121, 93	X			X			X			X			X			X			X			X			X			X			X		
37	24.70	N,N'-bis(2-phenylethyl)oxamide	X			X			X			X			X			X			X			X			X			X			X		
39	25.7	N-(2-ethoxyphenyl)-N-(2-ethylphenyl)oxamide	X			X			X			X			X			X			X			X			X			X			X		
40	26.64	N,N'-bis(2-ethoxyphenyl)oxamide	X			X			X			X			X			X			X			X			X			X			X		

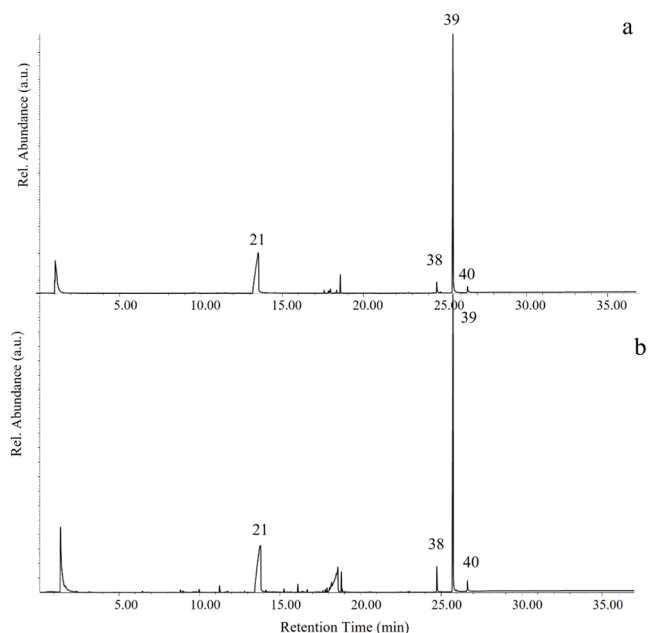


Fig. 6. Desorption step of double-shot Py-GC/MS of Paraloid® B44 coatings with 5% w/w AEDTA and Tinuvin® 312, unaged (a) and after 1000h of ageing (b).

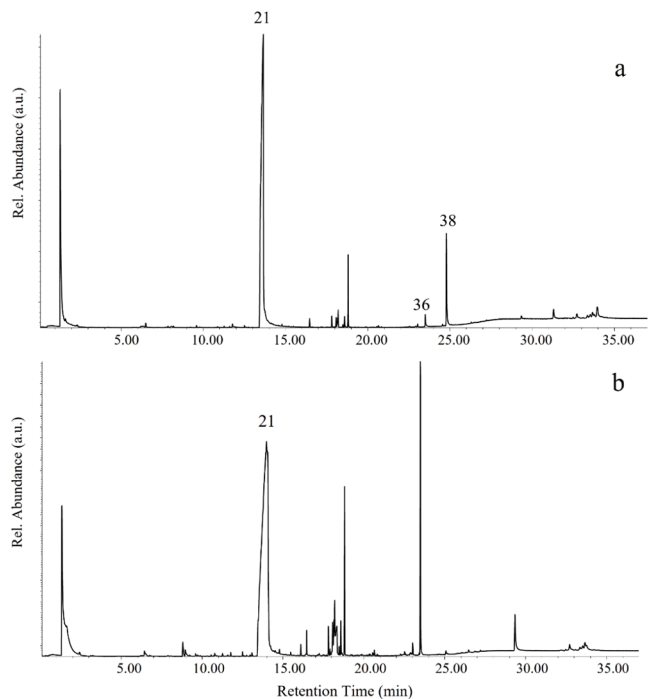


Fig. 7. Desorption step of double-shot Py-GC/MS of Paraloid® B44 coatings with 5% w/w AEDTA and Tinuvin® 5050, unaged (a) and after 1000h of ageing (b).

turn yellow over time.

Both inhibitors make Paraloid more brittle and decrease its reversibility, however the presence of light stabilizers mitigates these problems by reducing both the glass transition temperature variation over time and the percentage of insoluble material. This is especially true for coatings with AEDTA and light stabilizers.

Overall, Paraloid® B44 is confirmed to be stable to aging as there is no evidence of oxidation in the FTIR analyses, however both inhibitors

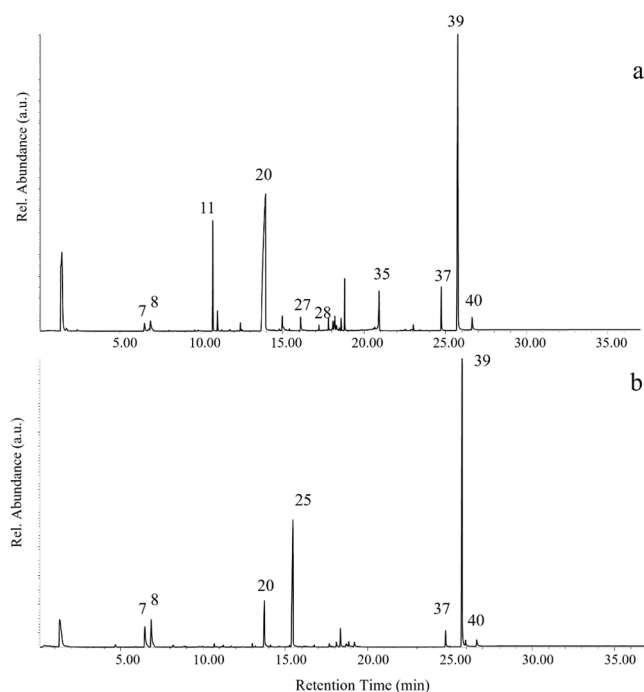


Fig. 8. Desorption step of double-shot Py-GC/MS of Paraloid® B44 coatings with 5% w/w MPT and Tinuvin® 312, unaged (a) and after 1000h of ageing (b).

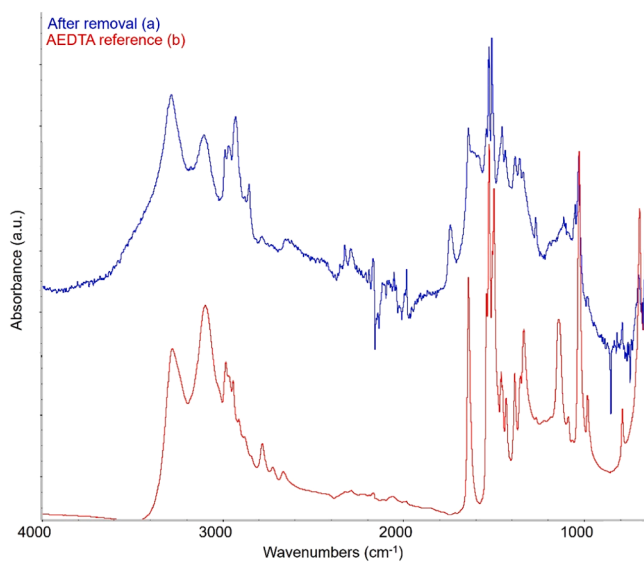


Fig. 9. FTIR spectrum of the bronze mock up after peeling off the coating (a) and AEDTA reference spectrum (b).

dispersed in it tend to leave the coating over time. Furthermore, MPT is not stable under solar light aging, in fact the Py-GC/MS marker peaks of this inhibitor after aging are not exactly the same as unaged samples or have very low intensities. The same can be said for BTA and Tinuvin® 5050. Conversely, AEDTA and Tinuvin® 312 are more stable over time.

Finally, the comparison between coatings applied on glass and on bronze demonstrates that inhibitors interact preferentially with bronze, probably through formation of Cu-inhibitor complexes, which attenuate the problem of the inhibitor release into the environment.

In particular, in the Paraloid coatings modified with AEDTA and applied on bronze discs, a layer of AEDTA adsorbed on the metal surface was detected at the bronze-coating interface, which appears to be an ideal stratigraphy to ensure effective anticorrosion activity to the acrylic

coating.

In conclusion, Paraloid® B44 modified with AEDTA 5% w/w and Tinuvin® 312 is the coating with the best performance in terms of stability of chemical and physical properties. The study here reported shows that the corrosion inhibitor AEDTA is stable over time and, even when embedded in a polymer matrix, it tends to concentrate on the bronze surface and to remain in the coating longer than other inhibitors such as MPT and BTA. One of the aspects that deserves to be explored in the future is the influence of the application method since the protective performance of the coating can be influenced by the thickness, number of layers and drying time [34]. Further studies are now underway aimed at evaluating the effective applicability and anticorrosive efficacy of the coatings here described on patinated bronze surfaces such as those found in outdoor works of art.

Declaration of Competing Interest

The authors declare that they have no known competing financial interests or personal relationships that could have appeared to influence the work reported in this paper.

Data availability

Data will be made available on request.

Acknowledgments

This research contributed to setting up the coatings and analytical procedures for the PRIN 2022 Project InCARE - Innovative multi analytical Characterisation of the influence of pAtina-coating interaction on anti-corrosive properties, funded by MUR. D. Scalrone and G. Pellis acknowledge support from the Project CH4.0 under the MUR program "Dipartimenti di Eccellenza 2023-2027" (CUP: D13C22003520001).

Supplementary materials

Supplementary material associated with this article can be found, in the online version, at [doi:10.1016/j.polymdegradstab.2023.110575](https://doi.org/10.1016/j.polymdegradstab.2023.110575).

References

- [1] A Artesani, F Di Turo, M Zucchelli, A. Traviglia, Recent advances in protective coatings for cultural, *Coatings* 10 (217) (2010), <https://doi.org/10.3390/coatings10030217>.
- [2] B Salvadori, A Cagnini, M Galeotti, S Porcinai, S Goidanich, A Vincenzo, C Celi, P Frediani, L Riosi, M Frediani, G Giuntoli, L Brambilla, R Beltrami, S. Trassatti, Traditional and innovative protective coatings for outdoor bronze: application and performance comparison, *J. Appl. Polym. Sci.* 135 (12) (2018), <https://doi.org/10.1002/app.46011>.
- [3] M Baglioni, G Poggi, D Chelazzi, P. Baglioni, Advanced materials in cultural heritage conservation, *Molecules* 26 (13) (2021), <https://doi.org/10.3390/molecules26133967>.
- [4] P. Letardi, Testing new coatings for outdoor bronze monuments: a methodological overview, *Coatings* 11 (2) (2021) 1–16, <https://doi.org/10.3390/coatings11020131>.
- [5] D A Scott, *Metallography and Microstructure in Ancient and Historic Metals*, Getty Conservation Institute in association with Archetype Books, Marina del Rey, CA, 1991. hdl.handle.net/10020/gci_pubs/metallography_microstructure.
- [6] H. Strandberg, Reactions of copper patina compounds - Influence of some air pollutants, *Atmos Environ.* 32 (20) (1998) 3511–3520.
- [7] G Giuntoli, L Rosi, M Frediani, B Sacchi, B Salvadori, S Porcinai, P. Frediani, Novel coatings from renewable resources for the protection of bronzes, *Prog. Org. Coat.* 77 (4) (2014) 892–903, <https://doi.org/10.1016/j.porgcoat.2014.01.021>.
- [8] Cano E, Lafuente D. 26 – Corrosion inhibitors for the preservation of metallic heritage artefacts, in: Dillmann P, Watkinson D, Angelini E, Adriaens A editors., vol 65: European Federation of Corrosion (EFC) Series. Eds. Woodhead Publishing in Materials, 2013. pp. 570–594. doi: 10.1533/9781782421573.5.570.
- [9] K Fent, G Chew, J Li, E. Gomez, Benzotriazole UV-stabilizers and benzotriazole: Antiandrogenic activity in vitro and activation of aryl hydrocarbon receptor pathway in zebrafish eleuthero-embryos, *Sci. Total. Environ.* 482–483 (1) (2014) 125–136, <https://doi.org/10.1016/j.scitotenv.2014.02.109>.

- [10] L A Ellingson, T J Shedlosky, G P Bierwagen, E R de la Rie, L B Brostoff, The use of electrochemical impedance spectroscopy in the evaluation of coatings for outdoor bronze, *Stud. Conserv.* 49 (1) (2004) 53–62, <https://doi.org/10.1179/sic.2004.49.1.53>.
- [11] D L Moffett, Wax coatings on ethnographic metal objects: justifications for allowing a tradition to wane, *J. Am. Inst. Conserv.* 35 (1) (1996) 1–7, <https://doi.org/10.1179/019713696806124557>.
- [12] T Kosec, Ž Novak, E Š Fabjan, L Škrlep, A Sever Škapin, P. Ropret, Corrosion protection of brown and green patinated bronze, *Prog. Org. Coat.* (2021) 161, <https://doi.org/10.1016/j.porgcoat.2021.106510>.
- [13] T Kosec, L Škrlep, E Š Fabjan, A Sever Škapin, G Masi, E Bernardi, E Chiavari, C Josse, J Esvan, L. Robbiola, Development of multi-component fluoropolymer based coating on simulated outdoor patina on quaternary bronze, *Prog. Org. Coat.* 131 (2019) 27–35, <https://doi.org/10.1016/j.porgcoat.2019.01.040>.
- [14] M Mihelčić, L Slemenik Peršek, E Šest, I Jerman, C Giuliani, G Di Carlo, M Lavorgna, A K Surca, Development of solvent- and water-borne fluoropolymer protective coatings for patina-free bronze discs, *Prog. Org. Coat.* 125 (2018) 266–278, <https://doi.org/10.1016/j.porgcoat.2018.09.014>.
- [15] G Masi, C Josse, J Esvan, E Bernardi, C Martini, M C Bignozzi, L Škerlp, E S Fabjan, M Kosec T Aufray, L Robbiola, C. Chiavari, Micro-characterisation of innovative organic coatings applied for the protection of outdoor bronze monuments. EUROCORR 2017-The annual congress of the european federation of corrosion, in: *Proceedings of the 20th International Corrosion Congress and Process Safety Congress, 2017*.
- [16] G Monari, M Galeotti, M Matteini, B Salvadori, R Stifanese, P Traverso, S Vettori, P. Letardi, Protective treatments for copper alloy artworks: preliminary studies of sodium oxalate and limewater effectiveness against bronze disease, *Environ. Sci. Pollut. Res.* 30 (2023) 27441–27457, <https://doi.org/10.1007/s11356-022-24107-0>.
- [17] M T Molina, E Cano, B. Ramírez-Barat, Protective coatings for metallic heritage conservation: a review, *J. Cult. Herit.* 62 (2023) 99–113, <https://doi.org/10.1016/j.culher.2023.05.019>.
- [18] F Faraldi, E Angelini, C Riccucci, A Mezzi, D Caschera, S. Grassini, Innovative diamond-like carbon coatings for the conservation of bronzes, *Surf. Interface Anal.* 46 (10–11) (2014) 764–770, <https://doi.org/10.1002/sia.5367>.
- [19] D Watkinson, *Preservation of Metallic Cultural Heritage*, Elsevier, Oxford, 2010.
- [20] S De Luna M, G G Buonocore, Messina E GiulianiC, G Di Carlo, M Lavorgna, L Ambroio, G M Ingo, Long-lasting efficacy of coatings for bronze artwork conservation : the key role of layered double hydroxide nanocarriers in protecting corrosion inhibitors from photodegradation, *Angew Chem. Int. Ed* (2018) 7380–7384, <https://doi.org/10.1002/anie.201713234>.
- [21] D A Pillard, J S Cornell, D L DuFresne, M T Hernandez, Toxicity of benzotriazole and benzotriazole derivatives to three aquatic species, *Water Res.* 35 (2) (2001) 557–560, [https://doi.org/10.1016/s0043-1354\(00\)00268-2](https://doi.org/10.1016/s0043-1354(00)00268-2).
- [22] 4–8 September J Wolfe, R Grayburn, H Khanjian, A Heginbotham, A. Phenix, J. Bridgland, Deconstructing Incalac: A formulation study of acrylic coatings for the protection of outdoor bronze sculpture, in: *Proceedings of the ICOM-CC 18th Triennial Conference Preprints, Copenhagen, Paris, International Council of Museums, 2017, 4–8 September*. 0808.
- [23] R F Witzel, R W Burnham, J.W. Onley, Threshold and suprathreshold perceptual color differences, *JOSA* 63 (5) (1973) 615–625.
- [24] V. Horie, *Materials for Conservation: Organic Consolidants, Adhesives and Coatings*, Routledge, London, New York, 2011. Paperback edition of 2nd.
- [25] O Chiantore, M. Lazzari, Photo-oxidative stability of paraloid acrylic protective polymers, *Polymer* 42 (1) (2001) 17–27, [https://doi.org/10.1016/S0032-3861\(00\)00327-X](https://doi.org/10.1016/S0032-3861(00)00327-X) (Guildf).
- [26] M Lazzari, D Scalalone, G Malucelli, O. Chiantore, Durability of acrylic films from commercial aqueous dispersion: Glass transition temperature and tensile behavior as indexes of photooxidative degradation, *Prog. Org. Coatings* 70 (2) (2011) 116–121, <https://doi.org/10.1016/j.porgcoat.2010.11.002>.
- [27] O Chiantore, M. Lazzari, Characterization of acrylic resins, *Int. J. Polym. Anal. Charact.* 2 (4) (1996) 395–408, <https://doi.org/10.1080/10236669608033358>.
- [28] O Chiantore, L Trossarelli, M. Lazzari, Photooxidative degradation of acrylic and methacrylic polymers, *Polymer* 41 (5) (2000) 1657–1668, [https://doi.org/10.1016/S0032-3861\(99\)00349-3](https://doi.org/10.1016/S0032-3861(99)00349-3) (Guildf).
- [29] O Chiantore, D Scalalone, T. Learner, Characterization of artists' acrylic emulsion paints, *Int. J. Polym. Anal. Charact.* 8 (1) (2003) 67–82, <https://doi.org/10.1080/10236660304884>.
- [30] D Scalalone, M Lazzari, O. Chiantore, Acrylic protective coatings modified with titanium dioxide nanoparticles: Comparative study of stability under irradiation, *Polym. Degrad. Stab.* 97 (11) (2012) 2136–2142, <https://doi.org/10.1016/j.polydegradstab.2012.08.014>.
- [31] C Monticelli, G Fantin, G Di Carmine, F Zanutto, A. Balbo, Inclusion of 5-mercapto-1-phenyl-tetrazole into β -cyclodextrin for entrapment in silane coatings: An improvement in bronze corrosion protection, *Coatings* 9 (8) (2019), <https://doi.org/10.3390/coatings9080508>.
- [32] M Mihit, R Salghi, S El Issami, L Bazzi, B Hammouti, Ait Addi El, Kertit S. A study of tetrazoles derivatives as corrosion inhibitors of copper in nitric acid, *Pigment Resin. Technol.* 35 (3) (2006) 151–157, <https://doi.org/10.1108/03699420610665184>.
- [33] C Giuliani, M Pascucci, C Riccucci, E Messina, M Salzano de Luna, M Lavorgna, G M Ingo, G. Di Carlo, Chitosan-based coatings for corrosion protection of copper-based alloys: A promising more sustainable approach fo cultural heritage applications, *Progr. Organ. Coat.* 122 (2018) 138–146, <https://doi.org/10.1016/j.porgcoat.2018.05.002>.
- [34] M T Molina, E Cano, B. Ramírez-Barat, Testing protective coatings for metal conservation: the influence of the application method, *Herit. Sci.* 11 (94) (2023), <https://doi.org/10.1186/s40494-023-00937-0>.